

# Estimation of Stratospheric Age Spectrum from Chemical Tracers

Mark R. Schoeberl, Anne R. Douglass  
NASA Goddard Space Flight Center, Greenbelt, MD  
and  
Brian Polansky  
Science Systems Applications Inc.  
Greenbelt, Md.

## Abstract

We have developed a technique to diagnose the stratospheric age spectrum and estimate the mean age of air using the distributions of at least four constituents with different photochemical lifetimes. We demonstrate that the technique works using a 3D CTM and then apply the technique to UARS CLAES January 1993 observations of CFC11, CFC12, CH<sub>4</sub> and N<sub>2</sub>O. Our results are generally in agreement with mean age of air estimates from the chemical model and from observations of SF<sub>6</sub> and CO<sub>2</sub>; however, the mean age estimates show an intrusion of very young tropical air into the mid-latitude stratosphere. This feature is consistent with mixing of high N<sub>2</sub>O air out of the tropics during the westerly phase of the QBO.

## 1. Introduction

The concept of the age-spectrum for trace gas transport [Kida, 1983; Hall and Plumb, 1994] has improved interpretation of the processes that lead to the observed distribution of stratospheric and oceanic minor constituents. The age-spectrum (sometimes called the boundary Green's function in oceanography) is the probability distribution of transit times for irreducible parcels between the source and the sample point within the interior of the domain. The age-spectrum thus links the boundary sources of constituents with the distribution within the interior of the fluid domain.

The utility of the age-spectrum has been demonstrated for both the stratosphere [Vaugh and Hall, 2002] and the ocean [Wunsch, 2002, Haine and Hall, 2002]. The application of this concept to the ocean and the stratosphere results from the fact that the boundary source region can be easily localized. For the stratosphere the boundary source region is the tropical tropopause. For the ocean, the boundary source region is the bottom water formation region in the North Atlantic.

The age-spectrum, although easily computed using a numerical model, cannot be directly observed. Nonetheless, the age-spectrum leaves its fingerprints on the observed tracer distribution. For example, the measurement of a tracer whose concentration at the boundary increases linearly with time automatically provides the first moment of the age-spectrum – the mean age. In the stratosphere, both CO<sub>2</sub> and SF<sub>6</sub> observations have been used to estimate the mean age [Vaugh and Hall, 2002], and because of this property,

tracers with a linearly increasing source are sometimes called clock tracers. Long records of nearly-inert tracers can also be used to estimate the age-spectrum [Johnson et al. 1999] but we do not have long reliable records of most observed tracers.

Additional information on the age-spectrum can be obtained from non-clock tracers. Schoeberl et al. [2000] noted this possibility for stratospheric constituents, and Hall et al. [2002] have estimated the oceanic age-spectrum using pairs of tracers with different source histories. In this paper, we further develop a technique to estimate the stratospheric age-spectrum from chemically active tracers. The idea is simple. Tracers with different lifetimes provide information about a different part of the distribution of transit times. Short-lived tracers are sensitive only to the rapid transit times since they are depleted after spending a short time in the stratosphere while long-lived tracers are more sensitive to the longer transit times. With  $N$  tracers of different lifetimes we can obtain  $N$  pieces of information about the age-spectrum.

Our approach for reconstructing the stratospheric age-spectrum is as follows. The age-spectrum is assumed to follow the analytic solution of Hall and Plumb [1994]. This assumption has been verified by numerical models [Vaugh et al., 1997, Schoeberl et al., 2000, Vaugh and Hall, 2002]. Haine and Hall [2002] also used this approach to estimate ocean age-spectrum using observed tracers. However, we have modified the analytic age-spectrum by adding a tracer time lag that is required in the less diffusive stratospheric circulation.

To test our methodology, we use a stratospheric chemical transport model (CTM) to calculate the age-spectrum. We also compute the distribution of artificial tracers with a path independent lifetime and the distribution of chemically active tracers. We then exercise the age-spectrum reconstruction method by reproducing the age-spectrum using the model tracers. Next, we reconstruct the age-spectrum using the observed tracers from the Cryogenic Limb Array Etalon Spectrometer (CLAES) [Roche et al. 1993] and Halogen Occultation Experiment (HALOE) [Russell et al. 1993] instruments flown aboard the Upper Atmosphere Research Satellite (UARS). In the next section we briefly describe the methodology. Our results are described in the subsequent sections.

## 2.0 Computing the Model Age-spectrum

The simplest method to compute the age-spectrum is to release a pulse (a delta function) of stratospherically inert tracer at the tropopause and allow it to disperse throughout the domain. Tracer loss only occurs in the troposphere. At a given point within the model domain, the graph of the concentration versus time is equivalent to the PDF of transit times for a stationary circulation. Hall and Vaugh [1997] report the age-spectrum and mean age distributions for two general circulation models using this method.

It is important to recognize that for non-stationary flows the pulse-method of computing the age-spectrum cannot generate the instantaneous spectrum. For example, the pulse will travel through the tropical lower stratosphere first before propagating to the mid-latitude and polar stratospheres. Thus for non-stationary flows the resultant age-spectrum

in the tropics will characterize flow conditions at the beginning of the integration period. Likewise the spectrum of the extra-tropics will be characterized by flow conditions at the end of the integration period. As a result, calculations of the mean-age using the results from a pulse will not be equivalent to the mean age using a clock tracer.

The chemical transport model (CTM) used in this study has been described by Douglass et al. [2003] and Schoeberl et al. [2003]. The model resolution is  $2^\circ$  latitude by  $2.5^\circ$  longitude with 28 pressure levels extending to 0.65 hPa. The CTM is driven by the GEOS-4 general circulation model winds [Douglass et al., 2003]. The model shows good tropical isolation of the lower stratosphere and compares well with observed tracer fields [Douglass et al., 2003]. To get the age-spectrum numerically, we integrate this model forward for 20 years after initiating a one-day square wave pulse at the tropical tropopause. The spectrum results from sampling the model every 30 days from the beginning of the integration. We also integrate a clock tracer (a linearly increasing surface source) and a series of seven radioactive tracers with lifetimes of 0.1, 0.3, 0.5, 1.0, 3.0, 5.0, and 7.0 years. The radioactive tracers have path independent loss rates thus their concentration is only a function of the transit time from the tropical tropopause. All of the chemical and radioactive tracer experiments were run for 20 years.

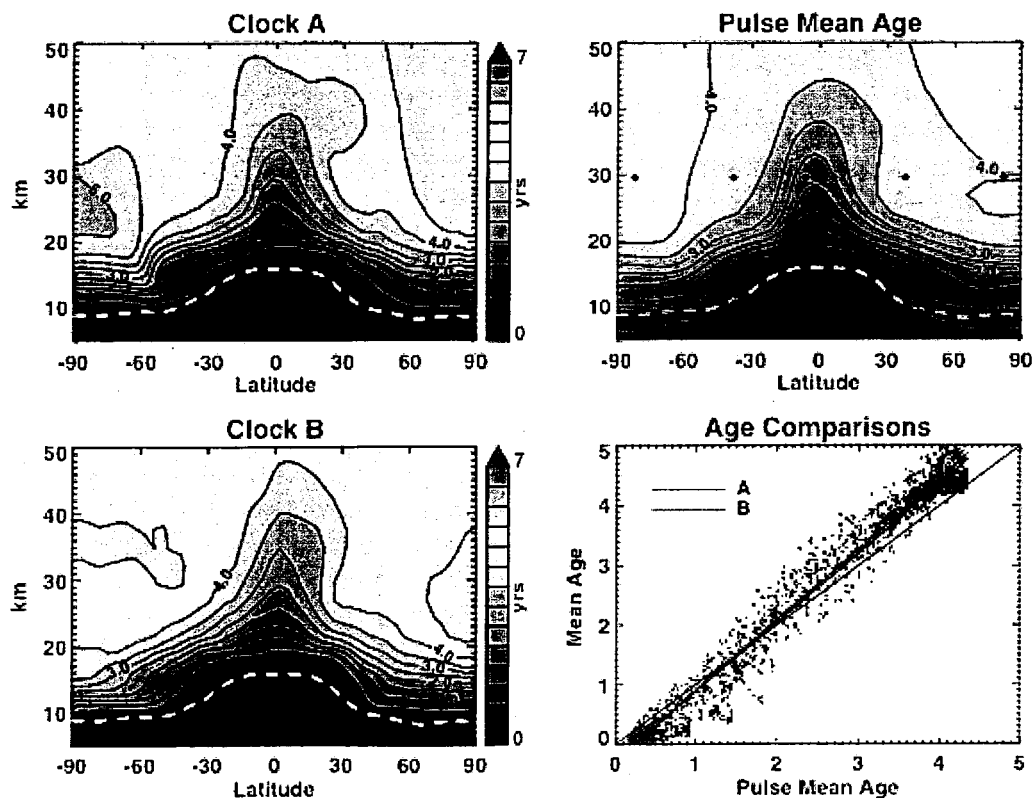


Figure 1 shows the results of a mean age calculation using two clock tracers (A and B) and the mean age computed from the pulse experiment. The two clock-tracer mean ages are plotted against the pulse experiment mean age in Figure 1d. See text for discussion. Small circles show the location of the spectra shown in Figure 2.

Figure 1 shows the mean age generated using the pulse and two clock-tracers. The mean age,  $\Gamma$ , is defined as

$$\Gamma = \int_0^{\infty} tG(x_0, x, t) dt \quad (1)$$

where  $G(x_0, x, t)$  is the Green's function or the age-spectrum. While the mean ages are similar in basic structure, there are some differences. The pulse mean age is younger than the clock tracer for the older clock ages and vice versa. The differences appear to result from the differences in forcing and the chemical loss. In the pulse experiment, the pulse originates at the tropopause. Chemical loss occurs below the tropopause so that air re-circulating back through the tropopause has no tracer concentration. The pulse cannot return to the stratosphere to influence the age.

The Clock A tracer value is incremented at the surface (except at the start where clock is set to the same value everywhere) with no chemical loss at the domain interior. For the Clock A tracer, it would seem possible that air could re-circulate through the tropopause back into the stratosphere and bias the oldest air to be even older. To test this idea, we performed a second clock experiment (Clock B) where the clock tracer value is reset to the current date within the troposphere at each time step. This Clock B experiment more closely resembles pulse experiment. Figure 1 shows that Clock B has younger air in the extremes than Clock A as predicted.

This result has an implication for connecting the mean age from clock tracers with the ages associated with other tracers. If the tracer is very inert, and has no tropospheric loss, then the mean age will be biased to slightly older values (about 6 months) compared to a tracer with a tropospheric loss. Thus the age deduced from inert tracers like  $\text{SF}_6$  is not exactly appropriate for estimating the concentration of non-inert tracers with lifetimes longer than roughly three years.

Returning to Figure 1 it is evident that for younger air, there is an additional bias between the pulse and clock experiments associated with air penetrating into the troposphere in the extra-tropics. For the pulse experiment, the pulse decays as it propagates into the troposphere due to the chemical loss localized to that region. For the Clock A and B experiments the continued forcing of the clock tracer tends to reset the tracer values toward young air creating the bias with respect to the pulse.

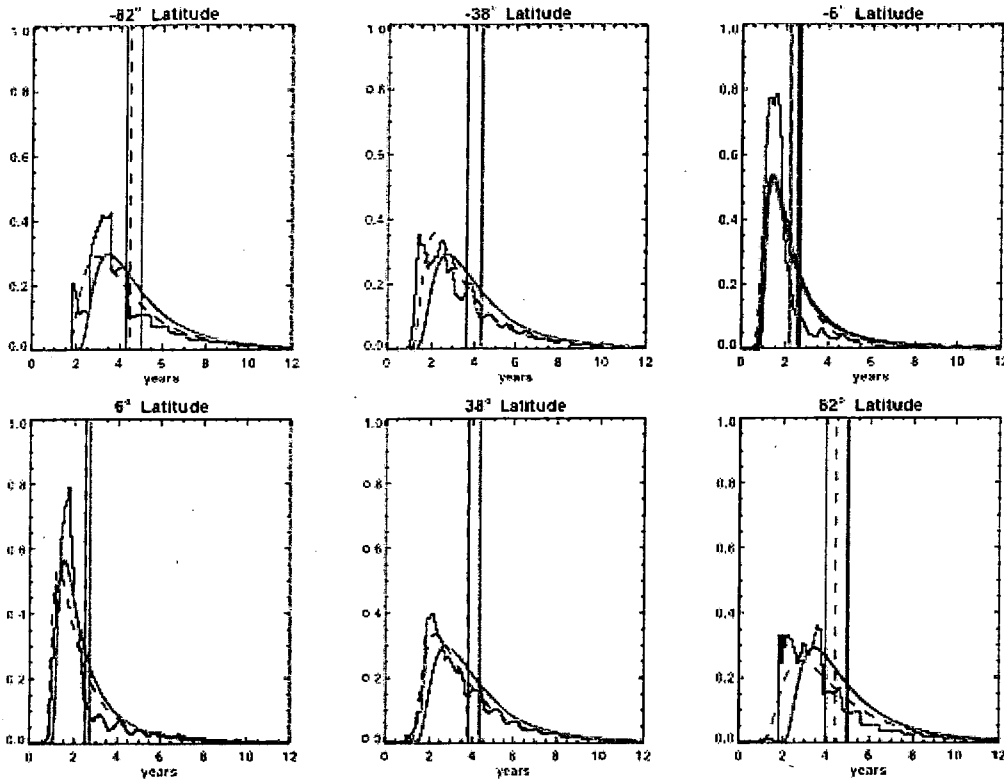


Figure 2. The age spectra from the model calculation at 30 km and the latitude indicated in the graph title. Locations are shown in Figure 1. Solid lines show the model spectra. Gray (smooth) and dashed lines show the fit spectrum using the radioactive tracers and the four chemical constituents, respectively. Vertical lines show the mean ages.

## 2.1 Radioactive tracers

To test the machinery of estimating the age-spectrum using tracers we begin with tracers whose decay rate is a function only of age. We call these “radioactive” tracers. Using the CTM we have run radioactive tracers with lifetimes of 0.1, 0.3, 0.5, 1.0, 3.0, 5.0 and 7.0 years. This spread was chosen to cover the mean ages shown in Figure 1. Using these tracers we assume that the age-spectrum,  $G$ , has the functional form

$$G = \frac{z}{2\sqrt{\pi K(t-t_{off})^3}} \exp\left(\frac{z}{2H} - \frac{K(t-t_{off})}{4H^2} - \frac{z^2}{4K(t-t_{off})}\right) \quad (2)$$

where  $z$  is the height of the sample point,  $H$  is the atmospheric scale height (7 km),  $K$  is the diffusion coefficient,  $t$  is the age and  $t_{off}$  is the age offset. This form is equivalent to the analytic expression derived by Hall and Plumb [1994] with the addition of the age offset. In the original 1D Hall and Plumb model,  $G$  has a value everywhere for  $t > 0$ . In model calculations, the age-spectrum is usually offset by some small age value because it takes a while for the pulse to arrive advectively, and the diffusion of the material ahead of

the pulse is not fast enough to produce an instantaneous response. Figure 2 illustrates this point, showing the pulse-generated age-spectrum at a variety of latitudes at 20 and 30 km. Note the age-spectrum offset at 30 km in the polar latitudes. We also note from Figure 2 that the age-spectrum generated by the model is quite similar to the analytic form.

To estimate the spectrum using tracers we use a multi-parameter least squares fit varying  $K$ ,  $z$ , and  $t_{\text{off}}$  to generate test values of  $G$ . We then search for the minimum of the function  $F$  where

$$F = \sum (\mu_i - \mu_i^*)^2 \quad (3a)$$

$$\mu_i^* = \int e^{-\lambda t} G(t, x, x_0) dt \quad (3b)$$

where  $\lambda$  is the radioactive decay rate (1/lifetime).  $F$  can be thought of as a score for the best overall fit to the data, but the simple least squares difference is not the only way to score the fit. For example,  $F$  could be based upon percentage differences from the analytic form. That type of score would give more weight to fitting the tail of the age-spectrum distribution. Tests using both types of scores show that the form given by (3a) usually gives the best overall mean ages when compared to observations (discussed below with Figure 9).

Figure 2 shows the spectrum fit generated using the radioactive tracers compared to the pulse generated spectrum at two altitudes and a series of latitudes. The mean ages are also shown. Overall the procedure and the analytic form capture the major structural features of the age-spectrum. Figure 3 shows a comparison of the mean age estimated from the radioactive tracers compared to the mean age computed from the pulse experiment. We note that the radioactive tracer fit produces a slight bias, tending to over estimate the age of the oldest air, but otherwise the fit seems to produce reasonable results. The modal age (age of the maximum in the age spectrum) estimated from the

radioactive tracers (not shown) also compares well with the pulse modal age.

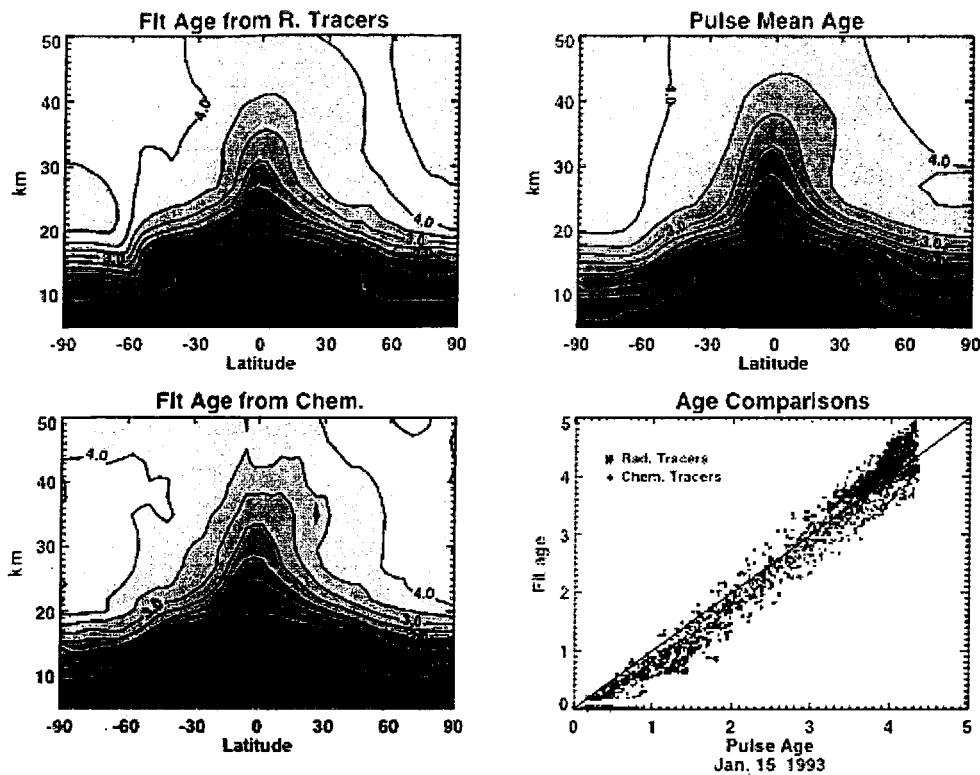


Figure 3 shows the mean age from the pulse experiment compared to the mean ages estimated from the radioactive tracers and the chemical tracers. Also see Fig. 2.

## 2.2 Chemical tracers

For chemical constituents, the amount of photochemical loss depends on the accumulated exposure to photolyzing radiation or locally generated reactive compounds such as OH. For such “total exposure constituents” [McIntyre, 1992], the 1:1 relation between age and trace gas amount is blurred, and parcels with the same age may have different trace gas amounts, depending on the latitude and altitude range of their paths. The local loss of the tracer by photolysis for species  $i$  can be written as  $J_i = \int \sigma_i F d\nu$  where  $F$  is the local solar flux and  $\sigma_i$  is the molecular cross section. The integral takes place over all frequencies,  $\nu$ . Because most long-lived tracers have cross sections with similar functional form, we can rewrite the expression above as  $J_i = \beta_i \int \sigma F d\nu$ . Now the photochemical exposure can be defined as  $dn = (\int \sigma F d\nu) dt$  so that  $d\mu = -\mu dn$  or in the case of OH loss  $d\mu/dt = -K\mu[OH]$  where  $[OH]$  is the hydroxyl concentration. If  $F$  were a constant, we would immediately recover the equivalent expression for the loss of a radioactive tracer. Schoeberl et al. [2000] showed that the average path approximation was valid for an ensemble of irreducible parcels with a given age. This approximation states that to first order we need consider only the average Lagrangian path of the irreducible fluid elements to the sample point, not the total spread of paths with same

ages. Furthermore, because  $F$  increases so rapidly with height, we need only consider regions near the end of the path. Thus we can thus approximate  $dn \approx \beta_i \bar{F}(y,z) \sigma dt$  where  $\bar{F}$  is the average flux over the ensemble of average paths. Combining terms gives

$$\mu_i = \int e^{-\lambda(y,z)t} G(t,y,z,y_o,z_o) dt \quad (4)$$

where  $\lambda(y,z) = \beta_i \bar{F}(y,z) \sigma$ . Thus the amount of the tracer is a function of the transit time with the loss coefficient a function of the final location. This result is consistent with Hall [2000] using the “leaky pipe” model of Neu and Plumb [1999]. Hall [2000] showed that the concentration of chemically active tracers was primarily a function of transit time because the longer transit times were simply resulted in higher path altitudes and thus more rapid photochemical loss.

### 2.2.1 Age-spectrum from Model Chemical Tracers

Since we know  $\mu_i$  from the photochemical model and  $G$  from the pulse experiment, we can solve for the value of the path integrated photochemical loss frequency,  $\lambda$  in (4). This solution is obtained numerically at each point varying  $\lambda$  until the mixing ratio matches the model. Note that the path integrated photochemical loss frequency is not the same as the local photochemical loss frequency although they may be close to each other in the tropics. We compute the path integrated photochemical loss frequency for four source gases, CFC-11, CFC-12,  $N_2O$  and  $CH_4$ , then using (3a and 3b) we can compute the age-spectrum. Figures 4-7 show the model values of the four trace gases and a computation of the same gases using (4). Values of  $\lambda^{-1}$  (roughly the decay time) are also shown in the figures. Note that  $\lambda^{-1}$  decreases rapidly with height in the tropics as expected from our approximations.  $\lambda^{-1}$  also decreases with latitude because the ensemble average path rises in the tropics and then falls at higher latitudes leaving the signature of the highest altitude (highest  $F$  value) on the value of  $\lambda$ . As expected  $\lambda^{-1}$  values are smaller (decay times are faster) for the shorter-lived tracers.

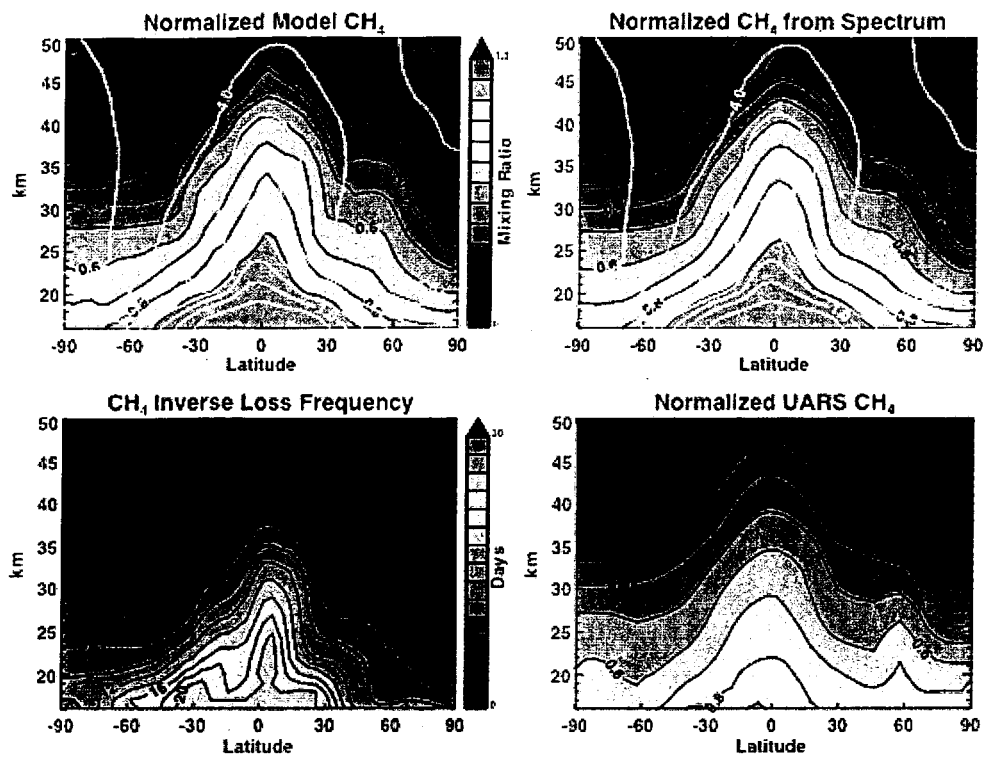


Figure 4. The top left panel shows the normalized chemical model values for CH<sub>4</sub> averaged for January normalized to the peak value. The lower left panel shows  $\lambda^{-1}$ . The upper right panel shows the computed tracer amount using the age spectrum and the path integrated loss frequency,  $\lambda$ . The mean age contours are shown over both upper figures in white. The lower right panel shows the monthly mean January 1993 value for CH<sub>4</sub> from UARS CLAES.

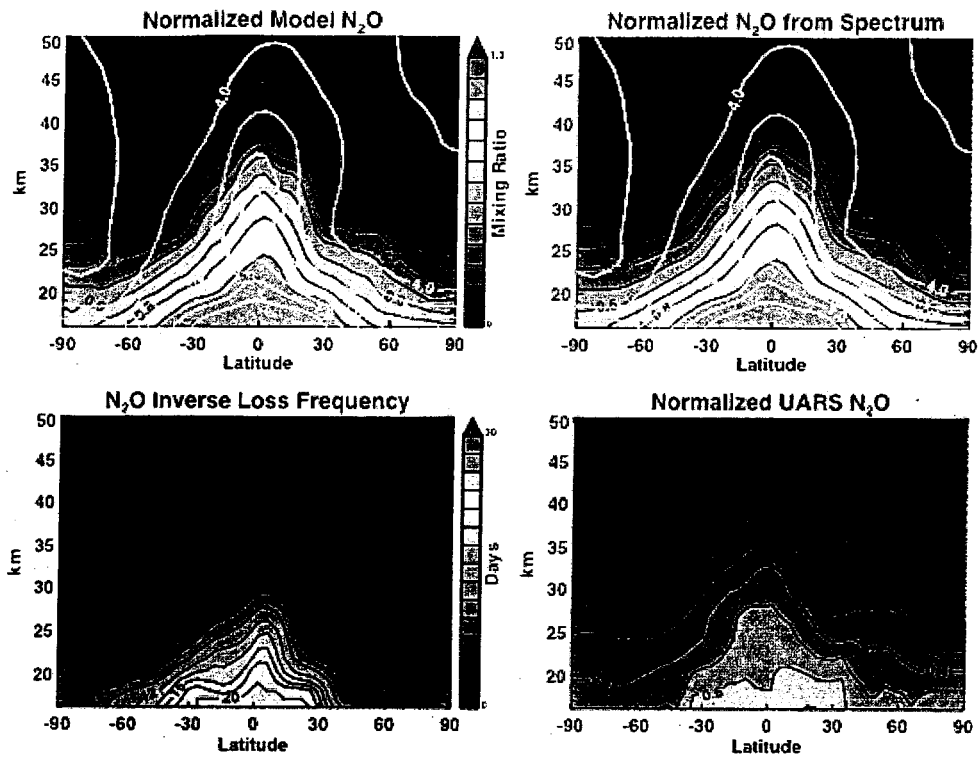


Figure 5. Same as Fig. 4 but for  $N_2O$ .

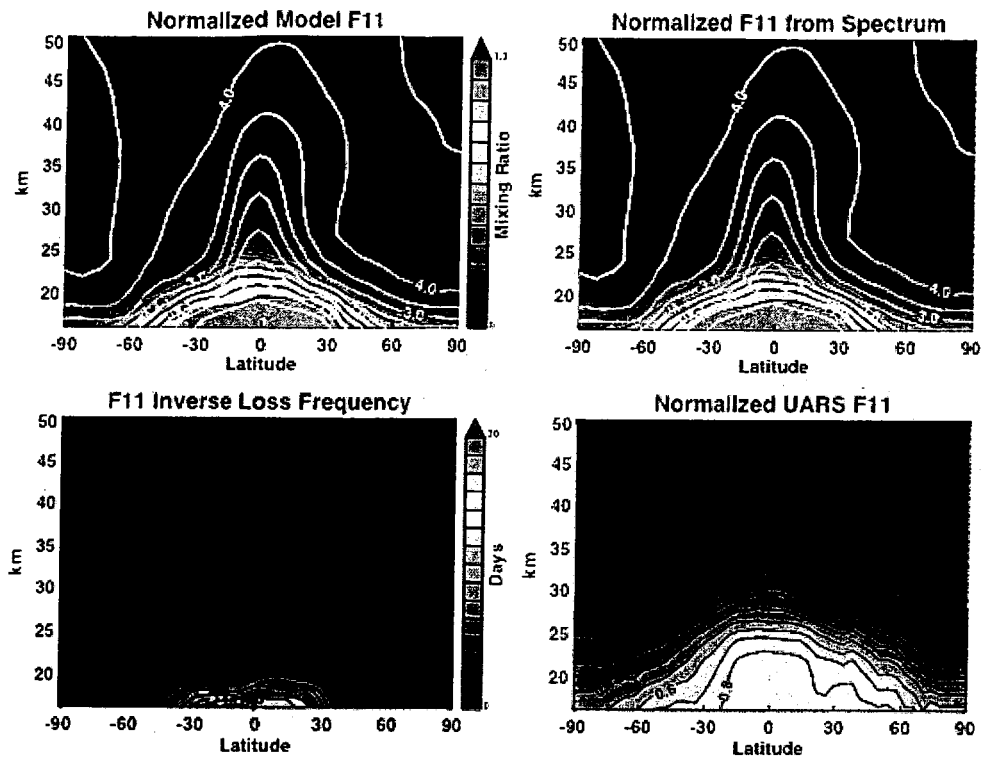


Figure 6. Same as Fig. 4 but for CFC11.

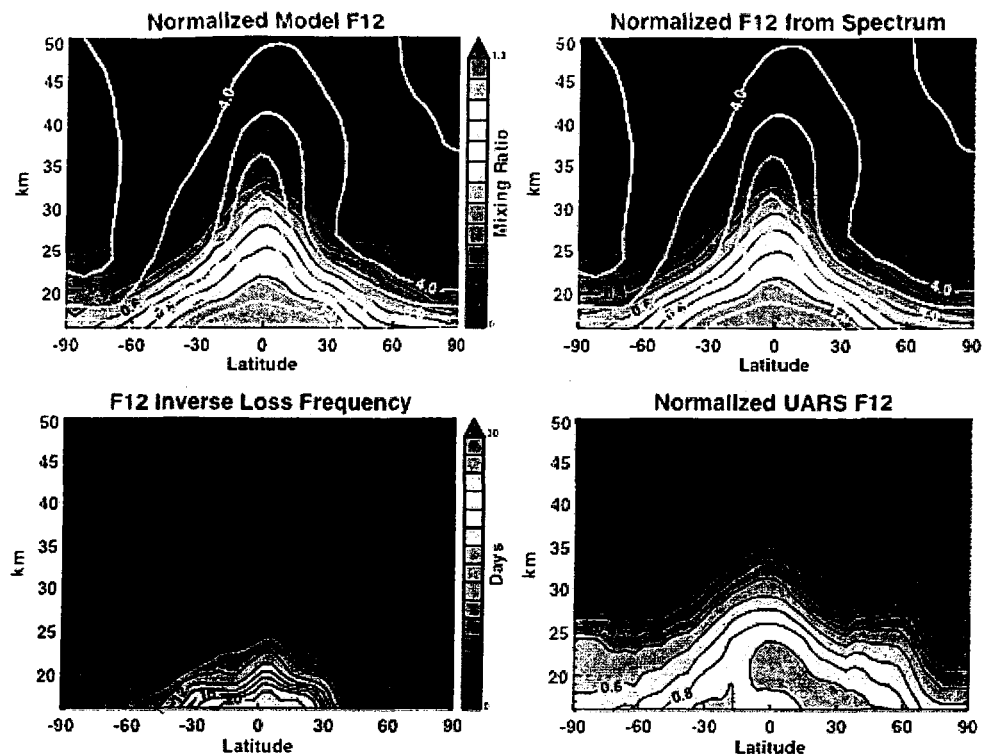


Figure 7. Same as Fig. 4 but for CFC12.

The mean age computed from the chemical tracer is shown in Figure 3. Our method produces a mean age that is quite comparable to the pulse and radioactive tracer mean age – although there is slightly more variability. Recall that with the radioactive tracer experiment we have seven tracers to constrain the three variables needed to estimate the age spectra. With the chemically active tracers, we only have four so it is not surprising that the fits are less tightly constrained. The sample age spectra generated using (3a) are shown in Figure 2. The agreement with both the pulse age spectra and the radioactive trace gas spectra is good.

### 2.2.2 Age estimates from UARS CLAES measurements

To estimate the age-spectrum from observations we must make the assumption that the  $\lambda$  values computed using the model are valid for the observed distributions as well. This assumption could be a small source of error. The error is small because the least squares fit to the multiple tracers tends to reduce errors associated with information from a single tracer. This is especially true in the lower stratosphere where all four tracers provide information on the age-spectrum. In the upper stratosphere or where the mean age is large, the age spectrum is less certain because the information is coming just from the longer-lived tracers  $\text{CH}_4$  and  $\text{N}_2\text{O}$ .

#### 2.2.2.1 Adjustments to the UARS CLAES data

We use the observations of CH<sub>4</sub>, CFC-11, CFC-12 and N<sub>2</sub>O from UARS Cryogen Limb Array Etalon Spectrometer (CLAES). The validation of CLAES observations is discussed in Roche et al. [1996] and Nightingale et al., [1996]. We focus on CLAES January 1993 observations, January 1993 includes a yaw cycle and both hemispheres are observed for approximately the same number of days. Near the tropical tropopause, the archived CLAES data shows local minima which are unrealistic compared to tropical balloon borne observations of N<sub>2</sub>O, CH<sub>4</sub> and other trace gases [Elkins et al., 1996; Ray et al., 1999; Boering et al. 1996; Andrews et al., 2001] and Halogen Occultation Experiment (HALOE) [Russell et al., 1993] observations for CH<sub>4</sub> [Park et al., 1996]. This anomaly is probably due to the interference of Pinatubo aerosol and tropical clouds in the retrieval algorithm. We adjust the data so that measurements only decrease with altitude in the tropics. Figures 4-7 show the adjusted normalized trace gas distributions used.

### 2.2.2.2 Age estimate

Figure 8 shows the mean age computed from UARS CLAES data compared to the mean age computed from the same tracers using the model. The mean age from the UARS data shows several distinct features – most dramatically the extension of very young air out of the tropical lower stratosphere into the Northern Hemisphere. The origin of this feature is clearly seen in the zonal mean N<sub>2</sub>O, CFC11 and CFC12 values which also show the extension northward out of the tropics (Fig, 6,7). O’Sullivan and Dunkerton [1997] noted this feature in CLAES N<sub>2</sub>O. They attributed it to the additional tropical mid-latitude eddy interaction during the westerly phase of the quasi-biennial oscillation (QBO) in the lower stratosphere. The numerical model does not exhibit a QBO so variations in isolation of the tropics with QBO phase are not produced in the model.

The age estimate from UARS data also shows significantly older air at high northern polar altitudes than the model. The origin of this feature is the very low values of methane and N<sub>2</sub>O in the upper stratosphere compared to the model (Figures 4 and 5). On the other hand, the southern hemisphere mid stratosphere is younger than the model estimated age. Here the UARS CLAES observations have higher values than the model, again consistent with our result.

Figure 9 compares the 20km mean ages composited by Waugh and Hall [2002] from a variety of sources with the mean ages computed here. First, the data sources for SF<sub>6</sub> and CO<sub>2</sub> are from individual balloon and aircraft flights and may vary in any individual year. None-the-less, the strong tropical isolation is a common feature as seen in the strong age gradient with latitude. The model estimates of the mean age using the clock tracer and the radioactive and chemical tracers reasonably reproduce this feature. The age estimate using the CLAES data also show this feature in the Southern Hemisphere. The mean age in the Northern Hemisphere shows the intrusion of young air out of the tropics as discussed above.

Finally, Figure 10 compares the 30 km age spectrum from the model using the four tracers and the age spectrum diagnosed from the UARS data (see Figure 2). The

structure of the spectrum diagnosed from the observed tracers is quite similar to that calculated from model tracers with the exception of the highest north latitude point. Looking at the trace gas distributions, it is clear that only  $\text{CH}_4$  provides any information on the spectrum in this region, because at high northern latitude during winter, air has descended from the mesosphere and all of the other tracers have been photolyzed. Thus we have good agreement on the mean age but no information on the spectral width. Thus it seems evident that a good check on the physical realism of the solution is that as the air increases in age the spectral width (see Waugh and Hall, 2002) should increase as well.

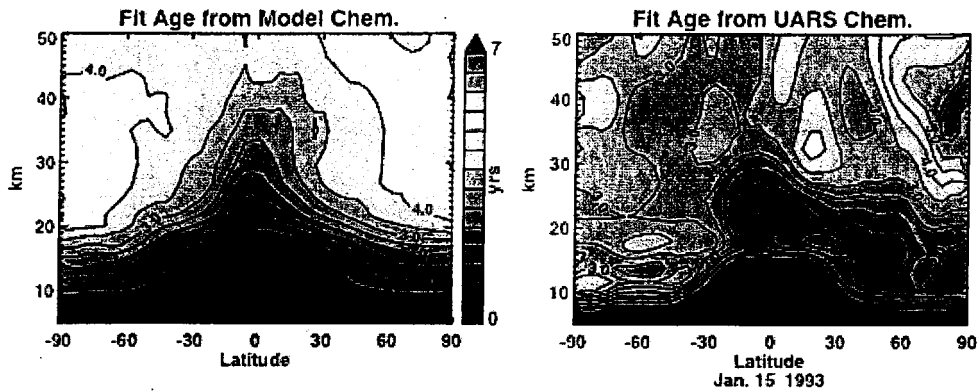


Figure 8 The mean age estimated using the four trace gases in the chemical model (I) and the mean age estimated from the same four tracers using UARS observations (®).

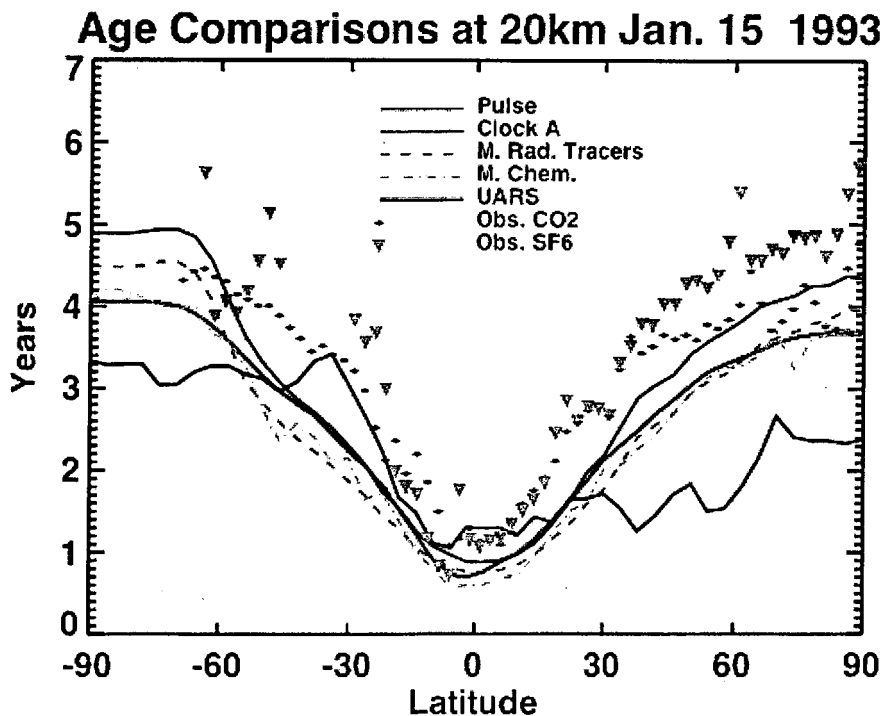


Figure 9. The 20 km mean age computed using the model and observations reported in Waugh and Hall [2002]. Observations are from the clock tracers  $\text{SF}_6$  (green) and  $\text{CO}_2$  (black) are shown as points. The mean ages are shown as lines for the various experiments, Pulse mean age (red),

Clock A tracer (blue), model radioactive tracers (cyan dashed), model chemical tracers (green dashed), UARS CLAES, black.

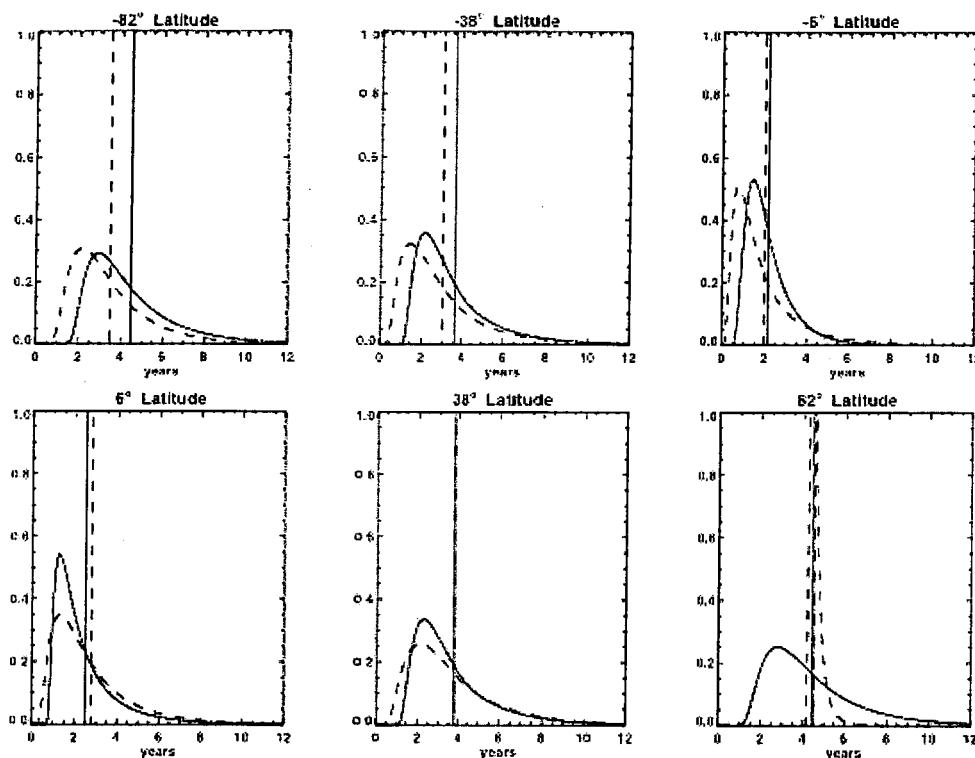


Figure 10. The 30 km age spectrum computed from the model using the four model chemical tracers (solid) and from UARS CLAES data (dashed). The vertical lines show the mean ages. A map of the mean ages is shown in Figure 8.

### 3.0 Summary and Discussion

A number of studies have sought to produce an estimate of the mean age of the stratosphere to diagnose the circulation and to test models. However, the mean age is just the first component of the age spectrum and for trace gases with finite chemical lifetime, the age spectrum itself is more useful. Depending on their lifetime, these chemically active gases may not be sensitive to the tail of the transit time distribution, which often strongly weights the first moment. Thus it would be useful to estimate the age spectrum from observed trace gases, and that is the goal of this study.

Using a multiple parameter least-squares fit we have derived an age-spectrum from trace gas measurements. Hall et al. [2002] has used the same approach to estimate the age of deep ocean water from tracers. Our approach differs from Hall et al. [2002] in that we use a 3 parameter model of the spectrum and we use chemically active tracers rather than tracers with differing source histories. We first test the approach by generating an age-spectrum using a 3D GCM and then recovering the spectrum with tracers that have a path independent decay rate. We then test the method with chemically active tracers from the model. Because we do not have path information for the real atmosphere we assume that

the chemical loss rate for the tracers is only a function of transit time. We argue that this approximation is reasonable since the photochemical loss increases with altitude so rapidly that longer transit times basically means that the irreducible parcels are reaching a higher altitude Hall [2000]. The parameterized chemical loss is computed from the model age-spectrum and trace gas concentration for CH<sub>4</sub>, N<sub>2</sub>O, CFC11 and CFC12.

After testing our approach using the model radioactive tracers and then chemical tracer, we extend our analysis to UARS CLAES observations for January 1993. The UARS data show significantly higher N<sub>2</sub>O, CFC11 and CFC12 concentrations at mid-latitudes than the model and, as a result, our computed mean age is younger than suggested by the observations composited by Waugh and Hall [2002]. O'Sullivan and Dunkerton [1997] noted this unusual feature in the CLAES data as well and they attributed additional tropical-mid-latitude mixing associated with the westerly phase of the QBO. This result suggests that there may be more year-year age variation in the lower stratosphere than previously suspected.

The approach we have developed here provides a quantitative method for simultaneous interpretation of many trace gas measurements. Although we have used only four tracers, tests with the radioactive tracers suggest that more robust results would be obtained with additional tracers with different lifetimes including clock tracers. For example, the four tracers used here plus SF<sub>6</sub> and perhaps some even shorter-lived halocarbons would provide a useful basis set. These measurements could be obtained from ACE and Aura measurements of the stratosphere.

While the analytic form of the age-spectrum is somewhat simplified, trajectory and chemical transport model estimates of the age-spectrum [e.g. Schoeberl et al., 2002] show that the analytic form first suggested by Hall and Plumb [1994] with the addition of an offset captures most of the information. Of course once the age-spectrum is computed then additional constituents can be estimated from their time history and photochemical loss rate.

#### Acknowledgements

This work was performed while the first author spent a few months visiting Oregon State University. He would like to thank the College of Ocean and Atmospheric Sciences for their hospitality and faculty for their interest.

#### References

- Andrews, A. E., et al., Mean ages of stratospheric air derived from in situ observations of CO<sub>2</sub>, CH<sub>4</sub>, and N<sub>2</sub>O, *J. Geophys. Res.*, 106, 32,295–32,314, 2001b.
- Boering, K. A., S. C. Wofsy, B. C. Daube, H. R. Schneider, M. Loewenstein and J. R. Podolske, Stratospheric transport rates and mean age distributions derived from observations of atmospheric CO<sub>2</sub> and N<sub>2</sub>O, *Science*, 274, 1340-1343, 1996.

Douglass, A. R., M. R. Schoeberl and R. B. Rood, Evaluation of transport in the lower tropical stratosphere in a global chemistry and transport model, *J. Geophys. Res.*, 108, doi:10.1029/2002JD002696, 2003.

Elkins, J. W. et al., Airborne gas chromatograph for in situ measurements of long-lived species in the upper troposphere and lower stratosphere, *Geophys. Res. Lett.*, 101, 16757-16770, 1996.

Hall, T. M., Path histories and timescales in stratospheric transport: Analysis of an idealized model, *J. Geophys. Res.*, 105, 22,811–22,823, 2000.

Haine, T. W. N. and T. M. Hall, A generalized transport theory: Water-mass composition and age, *J. Phys. Oceanogr.*, 32, 1932-1946, 2002.

Hall, T. M., and R. A. Plumb, Age as a diagnostic of stratospheric transport, *J. Geophys. Res.* 99, 1059-1070, 1994.

Hall, T. M., T. W. Haine, and D. W. Waugh, Inferring the concentration of anthropogenic carbon in the ocean from tracers, *Global Biogeochem. Cycles*, 16, doi:10.1029/2001GB001835, 2002.

Johnson D. G., et al., Stratospheric age spectra derived from observations of water vapor and methane, *J. Geophys. Res.*, 104, 21,595–21,602, 1999.

Kida, H., General circulation of air parcels and transport characteristics derived from a hemispheric GCM, Part 2, Very long-term motions of air parcels in the troposphere and stratosphere, *J. Meteorol. Soc. Jpn.*, 61, 510-522, 1983.

McIntyre, M. E., Atmospheric Dynamics: Some fundamentals, with Observational Implications, in *The Use of EOS for the Study of Atmospheric Physics*, Proceedings of the International School of Physics, "Enrico Fermi" Course 115, G. Visconti and J. Gille, eds., North Holland, NY, 313-386, NATO Summer School, 1992.

Roche, A. E. et al., Validation of CH<sub>4</sub> and N<sub>2</sub>O measurements by the cryogenic limb array etalon spectrometer instrument on the Upper Atmosphere Research Satellite [CH<sub>4</sub> N<sub>2</sub>O], *J. Geophys. Res.*, 101, 9679-9710, 1996.

Nightingale, R. W. et al., Global CF<sub>2</sub>Cl<sub>2</sub> measurements by UARS cryogenic limb array etalon spectrometer: Validation by correlative data and a model, *J. Geophys. Res.*, 101, 9711-9736, 1996.

Neu, J. L., and R. A. Plumb, Age of air in "leaky pipe" model of stratospheric transport, *J. Geophys. Res.*, 104, 19,243–19,255, 1999.

O'Sullivan, D and T. J. Dunkerton, Influence of the quasi-biennial oscillation on the global constituent distributions, *J. Geophys. Res.*, 102, 21731-21743, 1997]

Park, J. H. et al. Validation of Halogen Occultation Experiment CH<sub>4</sub> measurements from the UARS, *J. Geophys. Res.*, 101, 10,183-10,204, 1996.

Ray, E. A., et al., Transport into the Northern Hemisphere lowermost stratosphere revealed by in situ tracer measurements, *J. Geophys. Res.*, 104, 26,565–26,580, 1999.

Roche, A. E., et. Al., Validation of CH<sub>4</sub> and N<sub>2</sub>O measurements by the cryogenic limb array etalon spectrometer instrument on the upper atmosphere research satellite. *J. Geophys. Res.*, 101, 9679-7710, 1996

Roche, A. E., et al., The cryogenic limb array etalon spectrometer (CLAES) on UARS: Experimental description and performance, *J. Geophys. Res.*, 98, 10763-10776, 1993.

Russell, J. M. et al., The halogen occultation experiment, *J. Geophys. Res.*, 98, 10777-10798, 1993.

Schoeberl, M. R., L. Sparling, A. Dessler, C. H. Jackman, and E. L. Fleming, A Lagrangian view of stratospheric trace gas distributions, *J. Geophys. Res.*, 105, 1537–1552, 2000.

Schoeberl M. R., A. R. Douglass, Z. Zhu, and S. Pawson, A comparison of the lower stratospheric age spectra derived from a general circulation model and two data assimilation systems, *J. Geophys. Res.*, 108, 4113, doi:10.1029/2002JD002652, 2003.

Waugh, D. W. and T. M. Hall, Age of stratospheric air: Theory, observations and models, *Revs. Of Geophys.*, 40, doi:10.1029/2000RG000101, 2002.

Waugh, D. W., et al., Three dimensional simulations of long lived tracers using winds from MACCM2, *J. Geophys. Res.*, 102, 21493-21514, 1997.

Wuench, C., Oceanic age and transient tracers: Analytical and numerical solutions, *J. Geophys. Res.*, 107,10.1029/2001JC000797, 2002.

## Popular Summary of "Estimation of Stratospheric Age Spectrum from Chemical Tracers"

This paper using a new technique shows how the stratospheric age spectrum can be derived using chemical observations. The technique is demonstrated using both model fields and UARS data. The age spectrum contains all of the dynamical information needed to estimate the stratospheric constituent distribution given the tropopause mixing ratio. Forming the age spectrum from observational data is a rational and quantitative way to understand the dynamics of the stratosphere from all the information available, not just a few long-lived species. The results are applicable to non-measured species and gives us insight into stratospheric dynamics. For example, this study shows that young air appears to be more abundant in the northern hemisphere, lower stratospheric winter than models show.